Computed Micro-Tomographic Evaluation of Glide Path with Nickel-Titanium Rotary PathFile in Maxillary First Molars Curved Canals

Damiano Pasqualini, DDS, Caterina Chiara Bianchi, MD,† Davide Salvatore Paolino, MS, PhD,‡ Lucia Mancini, PhD,§ Andrea Cemenasco, BSc,† Giuseppe Cantatore, MD, DDS,¶ Arnaldo Castellucci, MD, DDS,‖ and Elio Berutti, MD, DDS**

Abstract

Introduction: X-ray computed micro-tomography scanning allows high-resolution 3-dimensional imaging of small objects. In this study, micro-CT scanning was used to compare the ability of manual and mechanical glide path to maintain the original root canal anatomy. **Methods:** Eight extracted upper first permanent molars were scanned at the TOMOLAB station at ELETTRA Synchrotron Light Laboratory in Trieste, Italy, with a microfocus cone-beam geometry system. A total of 2,400 projections on 360° have been acquired at 100 kV and 80 μA, with a focal spot size of 8 μm. Buccal root canals of each specimen (n = 16) were randomly assigned to PathFile (P) or stainless-steel K-file (K) to perform glide path at the full working length. Specimens were then microscanned at the apical level (A) and at the point of the maximum curvature level (C) for post-treatment analyses. Curvatures of root canals were classified as moderate (≤35°) or severe (≥40°). The ratio of diameter ratios (RDRs) and the ratio of cross-sectional areas (RAs) were assessed. For each level of analysis (A and C), 2 balanced 2-way factorial analyses of variance ($P < .05$) were performed to evaluate the significance of the instrument factor and of canal curvature factor as well as the interactions of the factors both with RDRs and RAs. **Results:** Specimens in the K group had a mean curvature of 35.4° ± 11.5°; those in the P group had a curvature of 38° ± 9.9°. The instrument factor (P and K) was extremely significant ($P < .001$) for both the RDR and RA parameters, regardless of the point of analysis. **Conclusions:** Micro-CT scanning confirmed that NiTi rotary PathFile instruments preserve the original canal anatomy and cause less canal aberrations. *(J Endod 2012;38:389–393)*

Key Words

Computed micro-tomography scanning, glide path, nickel-titanium, nickel-titanium rotary instrumentation, PathFile

Nickel-titanium (NiTi) rotary instruments reduce operator fatigue, the time required for shaping, and the risk of procedural errors associated with root canal instrumentation (1, 2). Superelasticity properties enable NiTi rotary files to be placed in curved canals exerting less lateral forces on the canal walls and maintaining the original canal shape (3, 4). NiTi rotary tools have unique design properties in terms of cross-sectional shape, taper, tip, and the number and angle of flutes. These properties improve the shaping process without creating canal aberrations, particularly in narrow and severely curved canals (2). Preserving root canal anatomy represents a major issue difficult to overcome. Despite this, several studies showed that shaping outcomes with NiTi rotary instruments are generally predictable (5, 6). Coronal enlargement and manual or mechanical preflaring to create a glide path was shown to be the first step for a safer use of NiTi rotary instrumentation because it prevents fractures of torsion instruments and shaping aberrations (7–9). Recently, NiTi rotary PathFiles (PFs) (Dentsply Maillefer, Ballaigues, Switzerland) were introduced to improve mechanical glide path (7, 10). These instruments are more capable of maintaining the original canal anatomy and cause less aberrations and modifications of canal curvature compared with manual preflaring performed with stainless-steel K-files (KFs) (7). Of note, clinician's expertise did not appear to have a significant impact on outcome (7). A number of techniques were used to evaluate endodontic instrumentation (3), such as plastic models (11), histological sections (12), scanning electron microscopic studies (13), serial sectioning with Bramante technique (14), radiographic comparisons (15), and silicon impressions of instrumented canals (16). X-ray micro–computed tomography (CT) scanners are based on cone-beam geometry and are optimized to obtain nondestructive high-resolution (from 1 to 10s of micrometers) 3-dimensional (3D) imaging of small objects. The main component of this scanner is the microfocus x-ray source featuring a spot size of <50 μm (usually only a few microns). Differently from the medical CT scan, the specimen is mounted on a high-precision rotation stage and revolves around its own axis, whereas the x-ray source and the detector are steady. The 3D reconstruction of the data is usually based on the Feldkamp algorithm (17). The micro-CT scan has recently emerged as a powerful

From the *Department of Endodontics, University of Turin Dental School, Turin, Italy; †Department of Radiodiagnostics, University of Turin, Turin, Italy; ‡Department of Mechanics, Politecnico di Torino, Turin, Italy; §Sincrotrone Trieste S.C.p.A, Trieste, Italy; ¶Department of Endodontics, School of Dentistry, University of Verona, Verona, Italy; and ‖Department of Endodontics, School of Dentistry, University of Florence, Italy.

Drs Cantatore, Castellucci, and Berutti declare financial involvement (patent licensing arrangements) with Dentsply Maillefer with direct financial interest in the materials discussed in this article.

Address requests for reprints to Dr Damiano Pasqualini, via Barrili, 9–10134 Torino, Italy. E-mail address: damianox@mac.com

0099-2399/$ - see front matter

Copyright © 2012 American Association of Endodontists.

doi:10.1016/j.joen.2011.11.011

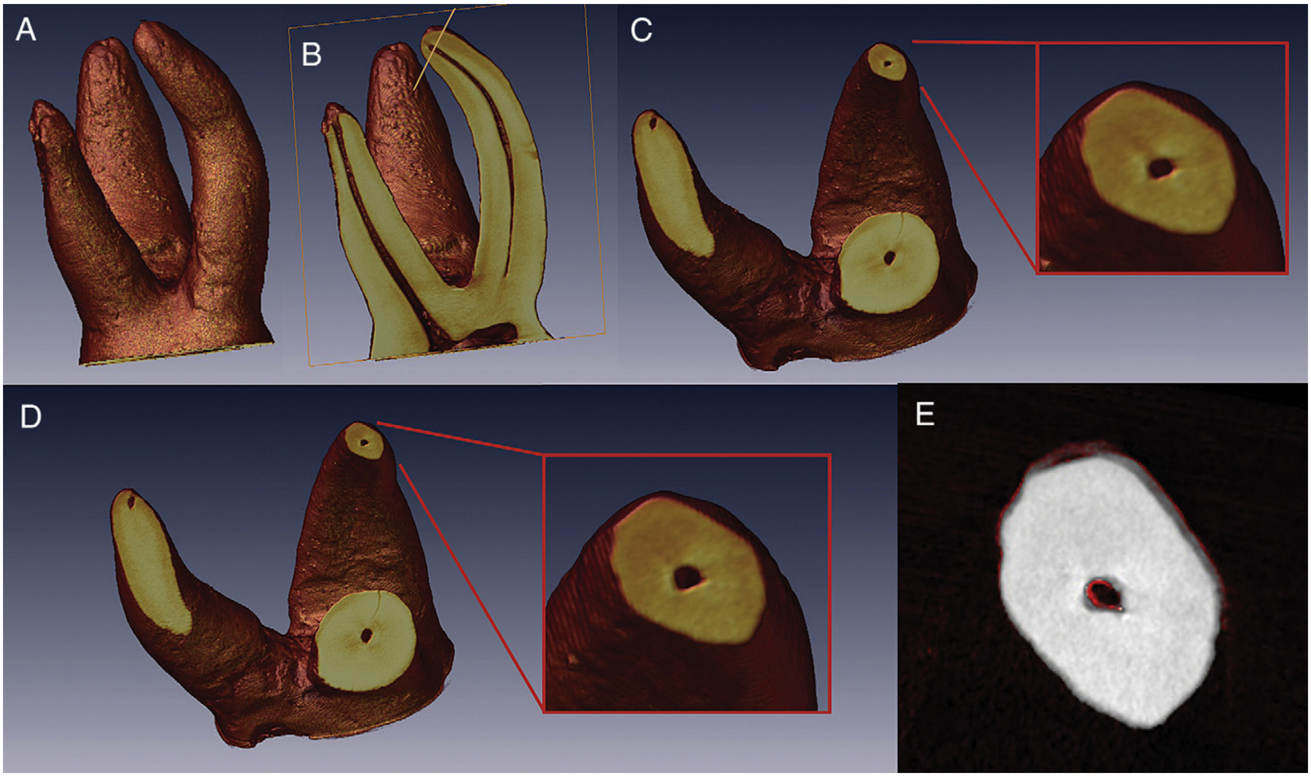

Figure 1. (*A*) A 3D reconstruction of a specimen. (*B*) The root canal path with selection of the cutting plane. (*C*) The cutting plane orthogonal to the canal axis in the pretreatment specimen. (*D*) The same cutting plane in the post-treatment specimen. (*E*) Image matching of the 2 radiologic sections, according to the previously selected cutting plane, shows the difference of the canal diameters between the pre- (*red*) and post-treatment (*gray*) specimens.

tool for the evaluation of root canal morphology. This noninvasive technique allows a detailed 3D evaluation of the effects of canal preparation on anatomy (18). It also allows the superimposition of 3D renderings of preoperative and postoperative canal system with a high resolution. In this study, we aimed to compare the ability of the manual and mechanical glide path to maintain the original root canal anatomy by using the micro-CT technique.

Materials and Methods

Eight extracted upper first permanent molars with a fully formed apex that had not undergone prior endodontic treatment were used. After debriding the root surface, specimens were immersed in a 5% solution of NaOCl (Niclor 5; OGNA, Muggiò, Italy) for 1 hour and then stored in saline solution.

Micro-CT Analysis

Specimens were mounted on a stable support and then scanned at the TOMOLAB station (19) at ELETTRA Synchrotron Light Laboratory in Trieste, Italy. The system is based on a cone-beam geometry with the following characteristics: (1) a sealed tungsten microfocus x-ray tube, with a focal spot size ranging from 5 to 40 μm, an energy ranging from 40 to 130 kV, and a maximum current of 300 microA and (2) a water-cooled charge-coupled device (CCD) camera with a large field of view (49.9 mm $\times$ 33.2 mm) and a small pixel size (12.5 $\times$ 12.5 μm). A total number of 2,400 projections on 360° at 100 kV and 80 μA, a focal spot size of 8 μm, with a focus-object and focus-detector distance of 110 mm and 300 mm, respectively, in a timeframe of 2 hours 32 minutes for each specimen was acquired.

Axial images were reconstructed by means of Cobra 7.2 software (Exxim, Pleasanton, CA) and subsequently elaborated for artifacts removal using PORE3D (20), a software developed at the ELETTRA research center. High-resolution raw 16-bit images were converted to an 8-bit TIFF file format; the whole stack gives a volume of around 1,000 $\times$ 1,000 $\times$ 1,000 isotropic voxels featuring a 9.2-μm side length. Each image stack was first equalized by ImageJ 1.43u 64 bit (a freeware software by the National Institutes of Health, Bethesda, MD) and then processed by Amira 5.3.3 64 bit edition (Visage Imaging, Richmond, Australia) for volume registration and cutting plane selection. The registration algorithm was based on the mean square difference between the gray values of the 2 image sets. The alignment steps have been set to 0.9 μm with a tolerance of 0.0001 units on the voxel intensity.

Each root canal path was studied dynamically by examining both high-resolution 3D rendering and orthogonal cross-sections. Root sections orthogonal to the canal axis were set at 2 different levels: at 1 mm from the canal apex (A) and at the point of maximum curvature (C). The cutting plane orientation was the same for both the pre- and post-treatment samples. This axial sections have been imported in TIFF format and analyzed with ImageJ to measure area, perimeter, and diameters (major and minor, orthogonal to one another) by using an automatic thresholding algorithm to avoid manual errors. Measurements were performed twice by the same operator (intraobserver control) and once by another operator (interobserver control).

Specimen Preparation

After access cavity preparation, the working length (WL) was established under microscopic vision (OPMI Pro Ergo; Carl Zeiss, Oberkochen, Germany) at 10× magnification when the tip of a #10 KF was visible at the root tip. Buccal root canals (MB1 and DB) of each specimen were randomly assigned to the PF test group or stainless-steel KF control group.

In the PF test group, the mechanical glide path was performed by using Glyde (Dentsply Maillefer, Ballaigues, Switzerland) as the lubricating agent with NiTi rotary instruments PF 1, 2, and 3 (Dentsply Maillefer) by using an endodontic engine (X-Smart, Dentsply Maillefer) with a 16:1 contra angle at the suggested setting (300 rpm on display, 5 Ncm) at the WL.

In the KF control group, the manual glide path was carried out by using Glyde as the lubricating agent with a stainless-steel KF #08-10-12-15-17-20 (Dentsply Maillefer) used with a "feed it in and pull" motion at the WL. During treatment, irrigation with 5% NaOCl (Niclor 5; OGNA, Muggiò, Italy) was performed with a 30-G needle syringe for a total of 10 mL. Root canals were dried with sterile paper points, and specimens were then microscanned as previously described for post-treatment analysis and comparisons (Fig. 1).

The angles of curvature of the canals were calculated and classified as moderate (M, ≤35°) or severe (S, ≥40°). To evaluate canal modifications induced by preparation, 2 different geometric parameters were considered for the statistical analysis: (1) the ratio of diameter ratios (RDRs) (ie, RDR = $[D/d]_{post}/[D/d]_{pre}$, where $[D/d]_{post}$ is the postpreparation ratio of the major diameter [D] to the minor diameter [d], and $[D/d]_{pre}$ is the prepreparation ratio of D to d and (2) the ratio of cross-sectional areas (RA) (ie, RA = A_{post}/A_{pre}, where A_{post} and A_{pre} are the postpreparation and the prepreparation cross-sectional areas, respectively).

For each level of analysis (A and C), 2 balanced 2-way factorial analyses of variance were performed to evaluate the significance of the instrument factor (PF and KF) and the canal curvature factor (M and S) at the 2 levels as well as the interactions of these factors both with the RDR and RA. To define RDR and RA parameters, 36 and 20 independent repetitions for each treatment combination were performed, respectively. The significance level was set to 5% ($P < .05$). All statistical analyses were performed by using the Minitab 15 software package (Minitab Inc, State College, PA).

Results

Specimens in the KF group had a mean curvature of 35.4° ± 11.5° (minimum = 20°, maximum = 55°), whereas specimens in the PF group had a mean curvature of 38° ± 9.9° (minimum = 25°, maximum = 55°). Four balanced 2-way factorial analyses of variance were performed, and the statistical significance of factors and interactions was evaluated by determining the following 12 P values: instrument factor: at point A, $P < .001$ for the RDR parameter and $P = .001$ for the RA parameter and at point C, $P < .001$ for both RDR and RA parameters; curvature factor: at point A, $P < .001$ for the RDR parameter and $P = .751$ for the RA parameter and at point C, $P = .045$ for the RDR parameter and $P = .011$ for the RA parameter; and instrument-curvature interaction: at point A, $P = .553$ for the RDR parameter and $P = .037$ for the RA parameter and at point C, $P < .001$ for the RDR parameter and $P = .025$ for the RA parameter. Therefore, the instrument factor was found to be extremely significant both for the RDR and RA parameters regardless of the point of analysis. The interval plots for the RDR parameter (Fig. 2*A*) and for the RA parameter (Fig. 2*B*) graphically confirm statistical significance of instrument factor. When PF is used, both the RDR and the RA parameters are closer to a value of 1, which means that canal modifications are statistically significantly reduced. The curvature factor significantly influenced both RDR and RA parameters except for RA assessed at the point of analysis A (Fig. 2). Finally, the interaction between factors significantly influenced the RDR and RA, again except for the RDR assessed at the point of analysis A (Fig. 3).

Discussion

Previous studies showed that micro-CT scans used to evaluate root canals prepared with NiTi hand or rotary instruments versus stainless-steel endodontic instruments provided a nondestructive and easy-to-repeat method (3, 21). Micro-CT scanning has been successfully used to evaluate the performance of ProTaper NiTi instruments (Dentsply Mailleffer) on shaping root canals despite varied anatomies (22). Data obtained with micro-CT scans enable the identification of morphologic changes associated with different biomechanical preparations including canal transportation, dentin removal, and final canal preparation (18, 23, 24). A major advantage of micro-CT scanning is the possibility to obtain highly accurate evaluation of root canal shape by the superimposition and measurement of 3D renderings (6, 18, 25). In the present study, micro-CT analysis confirmed the findings of a previous study showing that NiTi rotary PFs are more capable of maintaining original canal anatomy and cause less canal aberrations during instrumentation (7). Moreover, the impact of the instrument factor was significant in almost all interactions to canal curvature and point-of-

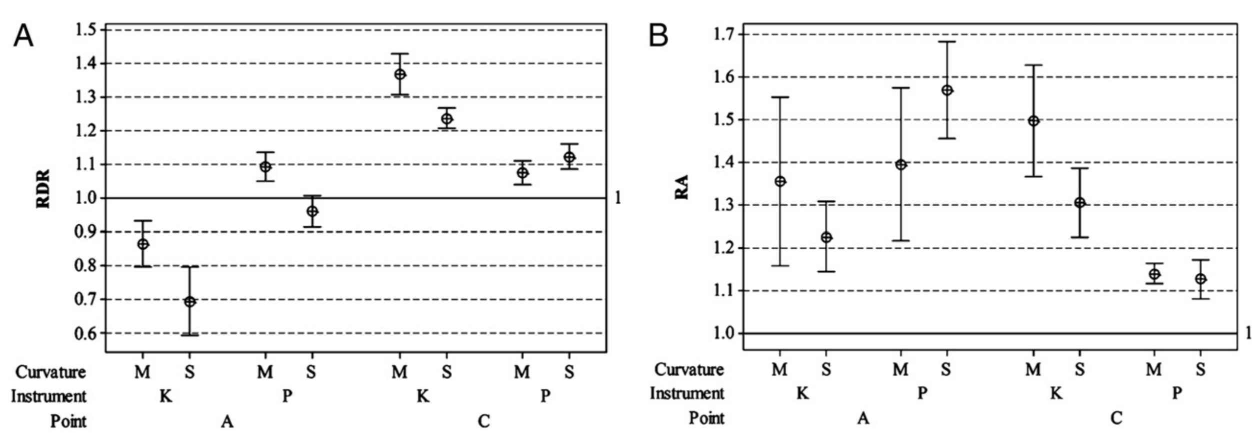

Figure 2. The interval plot for the RDR (*A*) and RA (*B*) parameters; 95% confidence intervals for the mean. A, canal apex; C, point of maximum canal curvature; K, K-file instrument; M, moderate curvature; P, PathFile instrument; S, severe curvature.

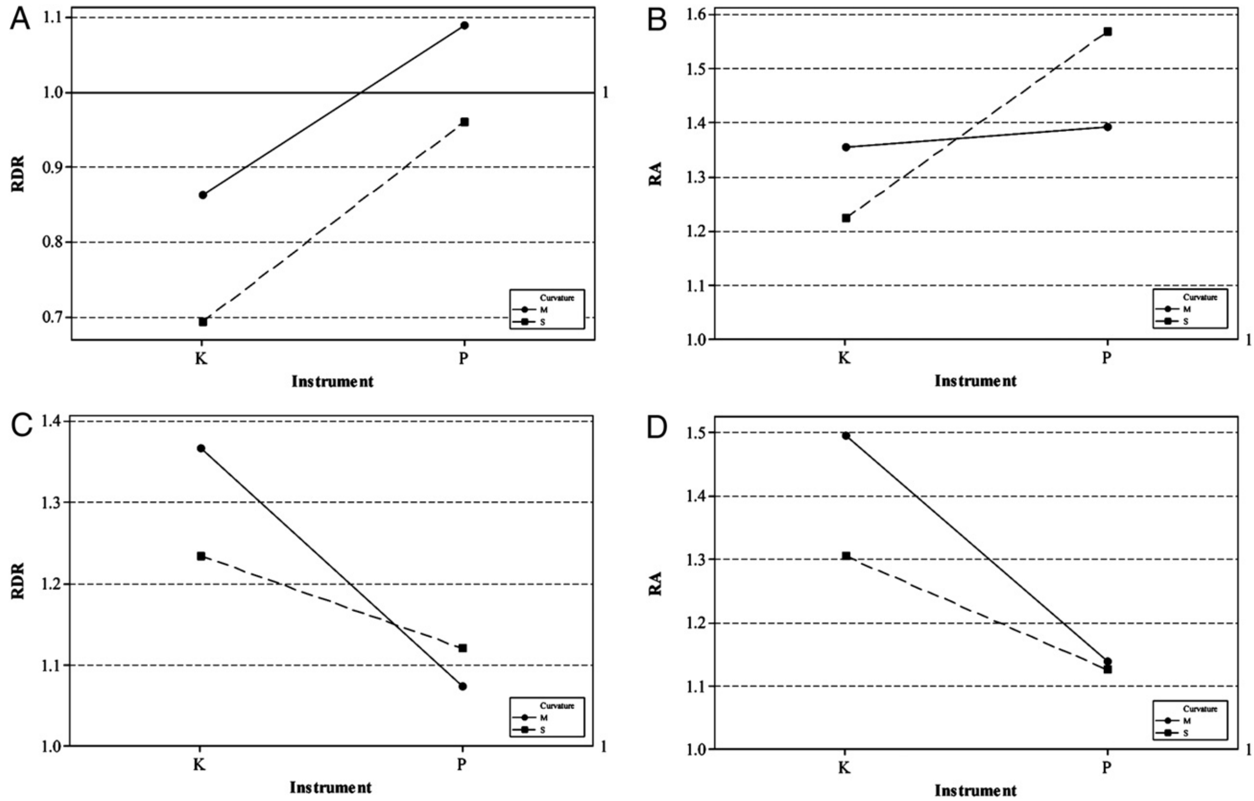

Figure 3. Interaction plots for each analysis of variance. (*A*) The RDR parameter evaluated at the canal apex (A). (*B*) The RA parameter evaluated at point A. (*C*) The RDR parameter evaluated at the point of maximum canal curvature (C). (*D*) The RA parameter evaluated at point C. Large nonparallelism between solid and dashed lines is evidence of statistical significance of interaction. K, K-file instrument; M, moderate curvature; P, PathFile instrument; S, severe curvature.

analysis factors considered. PF instruments caused significantly less alteration of the canal anatomy as evidenced by the analyses performed on the geometric variables. Preliminary manual or mechanical preflaring was shown to be fundamental before safe rotary instrumentation because it preserves rotary instruments from excessive torsion stresses (7–9, 26). Torsion stresses might increase dramatically if the area of contact between the dentine walls and the cutting edges of the instruments increases (27, 28) or if the canal section is smaller than the nonactive tip of the NiTi rotary instruments and the taper lock subsequently used (27–29). Maintaining the original canal shape using a less invasive approach is associated with better endodontic outcomes (6). Previous studies found that canal transportation leads to inappropriate dentine removal with a high risk of straightening of the original canal curvature and the formation of ledges in dentine wall as well as excessive apical enlargement with an hourglass appearance and subsequent defects in sealing (24, 30). Outer apical transportation and foramen widening may increase the risk of a lack of apical stop and extrusion of infected debris and microorganisms causing postoperative discomfort, thus jeopardizing endodontic treatment outcome (6,31–33). Studies showed that obturated root canals with irregular shapes leak significantly more compared with those with little or no canal transportation (34). Therefore, preserving the original canal shape and the lack of canal aberrations are associated with higher antimicrobial and sealing efficiency and do not excessively weaken tooth structure (35).

Within the limits of this study, our results confirmed that NiTi rotary PFs enable an optimal glide path for the NiTi rotary instruments used afterward. These instruments actually have high root canal centering ability and cause less modifications of the canal curvature and fewer canal aberrations. Therefore, PFs were shown to preserve the original canal shape considerably better than manual stainless-steel instruments.

Acknowledgments

The authors thank Dr D. Dreossi and F. Brun (Sincrotrone Trieste S.C.p.A) for their valuable support in micro-CT analysis and Dr Alovisi and Dr. Calissano (lecturers at the Department of Endodontics, University of Turin Dental School, Turin, Italy) for their active cooperation.

References

1. Javaheri HH, Javaheri GH. A comparison of three Ni-Ti rotary instruments in apical transportation. J Endod 2007;33:284–6.
2. Schäfer E, Vlassis M. Comparative investigation of two rotary nickel-titanium instruments: ProTaper versus RaCe. Part 2. Cleaning effectiveness and shaping ability in severely curved root canals of extracted teeth. Int Endod J 2004;37:239–48.
3. Gambill JM, Alder M, del Rio CE. Comparison of nickel-titanium and stainless steel hand-file instrumentation using computed tomography. J Endod 1996;22:369–75.
4. Coleman CL, Svec TA. Analysis of Ni-Ti versus stainless steel instrumentation in resin simulated canals. J Endod 1997;23:232–5.
5. Glossen CR, Haller RH, Dove SB, del Rio CE. A comparison of root canal preparations using Ni-Ti hand, Ni-Ti engine-driven, and K-Flex endodontic instruments. J Endod 1995;21:146–51.
6. Peters OA. Current challenges and concepts in the preparation of root canal systems: a review. J Endod 2004;30:559–67.
7. Berutti E, Cantatore G, Castellucci A, et al. Use of nickel-titanium rotary PathFile to create the glide path: comparison with manual preflaring in simulated root canals. J Endod 2009;35:408–12.
8. Patiño PV, Biedma BM, Liébana CR, Cantatore G, Bahillo JG. The influence of a manual glide path on the separation rate of NiTi rotary instruments. J Endod 2005;31:114–6.
9. Berutti E, Negro AR, Lendini M, Pasqualini D. Influence of manual preflaring and torque on the failure rate of ProTaper rotary instruments. J Endod 2004;30:228–30.

10. Gergi R, Rjeily JA, Sader J, Naaman A. Comparison of canal transportation and centering ability of twisted files, Pathfile-ProTaper system, and stainless steel hand K-files by using computed tomography. J Endod 2010;36:904–7.
11. Weine FS, Kelly RF, Lio PJ. The effect of preparation procedures on original canal shape and on apical foramen shape. J Endod 1975;1:255–62.
12. Walton RE. Histologic evaluation of different methods of enlarging the pulp canal space. J Endod 1976;2:304–11.
13. Mizrahi SJ, Tucker JW, Seltzer S. A scanning electron microscopic study of the efficacy of various endodontic instruments. J Endod 1975;1:324–33.
14. Bramante CM, Berbert A, Borges RP. A methodology for evaluation of root canal instrumentation. J Endod 1987;13:243–5.
15. Southard DW, Oswald RJ, Natkin E. Instrumentation of curved molar root canals with the Roane technique. J Endod 1987;13:479–89.
16. Abou-Rass M, Jastrab RJ. The use of rotary instruments as auxiliary aids to root canal preparation of molars. J Endod 1982;8:78–82.
17. Feldkamp LA, Davis LC, Kress JW. Practical cone-beam algorithm. J Opt Soc Am 1984;A1:612–9.
18. Peters OA, Laib A, Göhring TN, Barbakow F. Changes in root canal geometry after preparation assessed by high-resolution computed tomography. J Endod 2001;27:1–6.
19. TOMOLAB—X-ray CT laboratory, 2010. Available at: www.elettra.trieste.it/Labs/TOMOLAB.
20. Brun F, Mancini L, Kasae P, Favretto S, Dreossi D, Tromba G. Pore3D: A software library for quantitative analysis of porous media. Nucl Instrum Methods Phys A 2010;615:326–32.
21. Nair MK, Nair UP. Digital and advanced imaging in endodontics: a review. J Endod 2007;33:1–6.
22. Peters OA, Peters CI, Schönenberger K, Barbakow F. ProTaper rotary root canal preparation: effects of canal anatomy on final shape analysed by micro CT. Int Endod J 2003;36:86–92.
23. Paqué F, Ganahl D, Peters OA. Effects of root canal preparation on apical geometry assessed by micro-computed tomography. J Endod 2009;35:1056–9.
24. Loizides AL, Kakavetsos VD, Tzanetakis GN, Kontakiotis EG, Eliades G. A comparative study of the effects of two nickel-titanium preparation techniques on root canal geometry assessed by microcomputed tomography. J Endod 2007;33:1455–9.
25. Bjørndal L, Carlsen O, Thuesen G, Darvann T, Kreiborg S. External and internal macromorphology in 3D-reconstructed maxillary molars using computerized x-ray microtomography. Int Endod J 1999;32:3–9.
26. Roland DD, Andelin WE, Browning DF, Hsu GH, Torabinejad M. The effect of preflaring on the rates of separation for 0.04 taper nickel titanium rotary instruments. J Endod 2002;28:543–5.
27. Blum JY, Cohen A, Machtou P, Micallef JP. Analysis of forces developed during mechanical preparation of extracted teeth using Profile NiTi rotary instruments. Int Endod J 1999;32:24–31.
28. Peters OA, Peters CI, Schönenberger K, Barbakow F. ProTaper rotary root canal preparation: assessment of torque and force in relation to canal anatomy. Int Endod J 2003;36:93–9.
29. Yared GM, Bou Dagher FE, Machtou P. Influence of rotational speed, torque and operator's proficiency on ProFile failures. Int Endod J 2001;34:47–53.
30. Jafarzadeh H, Abbott PV. Ledge formation: review of a great challenge in endodontics. J Endod 2007;33:1155–62.
31. Siqueira JF Jr, Rôças IN, Favieri A, et al. Incidence of postoperative pain after intracanal procedures based on an antimicrobial strategy. J Endod 2002;28:457–60.
32. Seltzer S, Naidorf IJ. Flare-ups in endodontics: I. Etiological factors. 1985. J Endod 2004;30:476–81. discussion 475.
33. Vaudt J, Bitter K, Neumann K, Kielbassa AM. Ex vivo study on root canal instrumentation of two rotary nickel-titanium systems in comparison to stainless steel hand instruments. Int Endod J 2009;42:22–33.
34. Wu MK, Fan B, Wesselink PR. Leakage along apical root fillings in curved root canals. Part I: effects of apical transportation on seal of root fillings. J Endod 2000;26:210–6.
35. Moore J, Fitz-Walter P, Parashos P. A micro-computed tomographic evaluation of apical root canal preparation using three instrumentation techniques. Int Endod J 2009;42:1057–64.